Magnetism in two-dimensional $BN_{1-x}O_x$ and $B_{1-x}Si_xN$: Polarized itinerant and local electrons

Ru-Fen Liu[*] and Ching Cheng[†]

Department of Physics, National Cheng Kung University, 1 University Road, Tainan 70101, Taiwan
(Received 29 October 2009; revised manuscript received 10 February 2010; published 12 March 2010)

We use density-functional theory based first-principles methods to study the magnetism in a two-dimensional hexagonal BN sheet induced by the different concentrations of oxygen and silicon atoms substituting for nitrogen (O_N) and boron (Si_B), respectively. We demonstrate the possible formation of three distinct phases based on the magnetization energy calculated self-consistently for the ferromagnetic (ME_{FM}) and antiferromagnetic (ME_{AFM}) states, i.e., the paramagnetic phase with $ME_{FM}=ME_{AFM}$, the ferromagnetic phase with $ME_{FM}>ME_{AFM}$, and finally the polarized itinerant electrons with finite ME_{FM} but zero ME_{AFM}. While the O_N system was found to exist in all three phases, no tendency toward the formation of the polarized itinerant electrons was observed for the Si_B system though the existence of the other two phases was ascertained. The different behavior of these two systems is associated with the diverse features in the magnetization energy as a function of the oxygen and silicon concentrations. Finally, the robustness of the polarized itinerant electron phase is also discussed with respect to the O substitute-atom distributions and the applied strains to the system.

I. INTRODUCTION

The theoretical model of the two-dimensional (2D) homogeneous electron gas (HEG), which considers the electrons moving in a 2D uniform positive charge background, serves as an important model system for studying the fundamental many-electron behavior in 2D systems. These physical properties are closely connected to the operations of conduction electrons in the layered semiconductor devices as well as the recently synthesized 2D periodic systems.[1,2] The most creditable method considered presently for studying the 2D HEG is the quantum Monte Carlo[3–6] (QMC) method. The recent QMC studies found no region of stability for a ferromagnetic fluid in the 2D HEG.[6] The phases were found to transit directly from a polarized Wigner crystal[7] to the normal fluid (paramagnetic state). However, it would be interesting to explore the parallel phase diagram for real materials, i.e., systems of electrons moving in a neutralizing background formed by a 2D lattice of nuclei, and study the corresponding magnetic property as a function of the electron density.

Inspired by the exciting experimental works on the discovery and synthesization of hexagonal boron nitride (h-BN) in low-dimensional structures[1,2,8,9] as well as the possible formation of magnetism in these systems through creations of defects,[10,11] here we present density-functional theory (DFT) (Ref. 12) based first-principles studies on the magnetic properties of a 2D hexagonal BN sheet induced by the oxygen and the silicon atoms substituting for N and B atoms, respectively, (denoted as O_N and Si_B hereafter), i.e., $BN_{1-x}O_x$ and $B_{1-x}Si_xN$. We demonstrate the possible formation of polarized itinerant electrons in the O_N system. The stable phases are identified as, in increasing substitute-atom (SA) concentration x, the paramagnetic phase, the ferromagnetic phase, and finally the polarized itinerant electrons. In addition, the Si_B system which though supports the formation of ferromagnetic phase displays no tendency to the stabilization of the polarized itinerant electrons, i.e., resembling the QMC result for a 2D HEG.

II. COMPUTATION METHOD

The DFT calculations employed in the present study use the generalized gradient approximation[13] for the exchange-correlation energy functional and the projector-augmented-wave method[14,15] for describing the interaction between core and valence electrons as implemented in the VASP (Ref. 16) code. To simulate the systems with the substitute-atom concentration x ranging from 1/55 to 1/4, the supercells with distance (denoted as d_{nn}) of ~17.5, 13.3, 10, 7.5, and 5 Å between nearest-neighbor substitute atoms were constructed. A vacuum distance larger than 12 Å was used in the calculations to remove the interaction between layers. The numerical convergence was accomplished by using k-point meshes of (7 7 1) generated from Monkhost-Pack method[17] for the supercell consisting of 2×2 unit cells (and the similar density of k-point meshes for the supercells of other sizes), and the kinetic-energy cutoff of 400 eV (with tests at 500 eV) for expanding the single-electron Kohn-Sham wave functions in plane-wave basis. The atomic forces calculated by Hellmann-Feynman theorem[18] were relaxed to less than 0.02 eV/Å in all calculations. Furthermore, the volume and shape were also allowed to relax for the systems constructed by 2×2 ($x=1/4$ and $d_{nn}\sim5$ Å) and 3×3 ($x=1/9$ and $d_{nn}\sim7.5$ Å) supercells. We shall emphasize that the relaxed structures for O_N and Si_B are found to likely preserve its threefold symmetry in the hexagonal lattice at all studied substitution concentrations.[19] When switching on the spin-polarized calculations, the atomic forces were further relaxed.

III. RESULTS

The calculated magnetizations for both O_N and Si_B stay as $1\mu_B$ per substitute atom throughout the systems of fractional x's studied in this work.[20] The magnetic moment found in both systems can be attributed to the donated electrons accommodating at the bottom of the conduction band due to the presence of the substitute atoms which is confirmed by
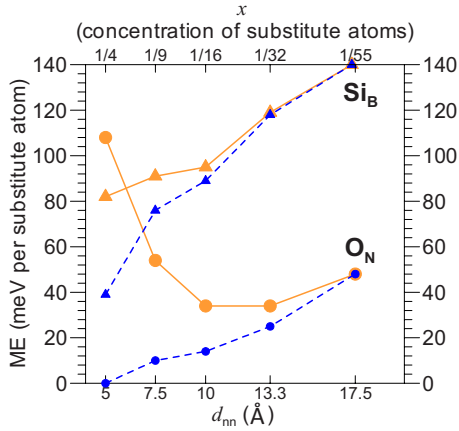
FIG. 1. (Color online) The magnetization energy ME$_{FM}$ (solid lines) and ME$_{AFM}$ (dashed lines) per substitute atom with respect to d_{nn} as well as the substitute-atom concentration x. The circles and triangles are for the systems of O$_N$ and Si$_B$, respectively.

the corresponding density of states (DOS) of these systems. The magnetization energies (MEs) for the ferromagnetic and antiferromagnetic configurations are defined as the energy gains of these configurations (E_{FM} and E_{AFM}) with respect to those obtained from the nonspin-polarized calculations (E_{NSP}), i.e., ME$_{FM}$=E_{NSP}−E_{FM} and ME$_{AFM}$=E_{NSP}−E_{AFM}, respectively. (All the magnetic-related quantities discussed in this work are given in the unit of per substitute atom.) Assuming that the interaction among the local magnetic moments in these magnetic systems can be approximately described by the nearest-neighbor Heisenberg Hamiltonian, H =−$\sum_{i>j}JS_iS_j$, then the interaction strength as well as the magnetic coupling types, i.e., ferromagnetism and antiferromagnetism, can be extracted from the exchange energy J =$\frac{1}{4}$(ME$_{FM}$−ME$_{AFM}$). Note that the initial magnetic configurations in calculating E_{AFM} were set up with antiparallel local moments of equal magnitude and then followed by the spin-density relaxation in the self-consistent calculations. In Fig. 1, we present the calculated magnetization energy of O$_N$ and Si$_B$ as a function of the substitute-atom concentration x. At low concentrations of $x \leq 1/55$, both systems are stabilized at paramagnetic phase, i.e., $J=0$ but with finite ME$_{FM}$ =ME$_{AFM}$ of around 50 meV for O$_N$ and 140 meV for Si$_B$. The presence of substitute atoms in these concentrations therefore introduces local moments into these systems yet no

interactions among them, i.e., isolated local moments. These moments were identified as mostly p_z-like and their locality was manifested from the narrow-bandwidth bands splitting from the original conduction band of the BN sheet. The spin density for Si$_B$ distributes mostly around the Si-atom sites while that for O$_N$ is considerably more extensive, i.e., up to the third-nearest-neighboring B atoms to the O atom.

As the substitute-atom concentration is increased, both systems develop into the ferromagnetic phase with finite J. The values of $4J$ can be as high as 42 meV for Si$_B$ at x =1/4, which corresponds to a Curie temperature estimated with the mean-field approximation (T_{CMF}) of 80 K and 44 meV for O$_N$ at x=1/9, to a T_{CMF} of 83 K. Note that these ferromagnetic systems consist of no magnetic elements such as Fe, Co, Ni, or rare-earth elements.

The most particular feature takes place at x=1/4 of O$_N$ when a finite ME$_{FM}$ is accompanied by a zero ME$_{AFM}$. That is, the initial antiparallel configurations in calculating E_{AFM} were found to relax to the nonspin-polarized state. The zero ME$_{AFM}$ together with a finite ME$_{FM}$ suggests the formation of polarized itinerant electrons in O$_N$, with an exchange split of 0.75 eV in bands.

The different characteristics of O$_N$ and Si$_B$ at x=1/4 are implied in the distinct band structures generated by the nonspin-polarized calculations. The band structure of hexagonal BN sheet has been shown previously[22] to display a nearly-free-electronlike characteristic around Γ point of the conduction band (CB). Since the most important contribution to determine the magnetic properties in O$_N$ and Si$_B$ comes from the electronic states near the Fermi level (E_F), we present in Fig. 2 the corresponding CBs for the BN sheet, and those for O$_N$ and Si$_B$ at x=1/4. In the BN sheet, only s electrons of N atoms contribute to the free-electronlike s band (blue diamonds) while the p_z band (red dots) is mainly from the p_z electrons of B atoms. When the O or Si substitute atoms are introduced into the system, the original s band and p_z band receive contributions from both B and O atoms in O$_N$ but from Si atom alone in Si$_B$. Relative to the generally inert α band (whose energy at Γ point is taken as the energy reference zero in Fig. 2), the effect of O and Si substitute atoms are primarily the shift of s and p_z bands and the change in dispersion of the p_z band. In O$_N$, the upward shifted s band and the downward shifted p_z band results in the joint of the two bands around the Γ point. The joint along with a relatively flatter p_z band provide an excellent condi-
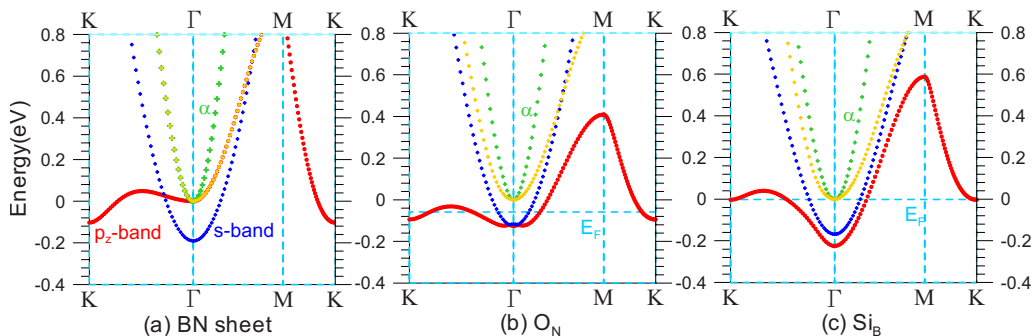

FIG. 2. (Color online) Band structures for (a) BN sheet and (b) O$_N$ (c) Si$_B$ calculated at x=1/4. The energy zero is taken to be the minimum of the band α's (green crosses).

tion for high DOS at E_F which further leads to the formation of polarized itinerant electrons. In Si_B, the main effect is the pressed downward p_z band to below the almost unaltered s band with, contrary to that in O_N, a more dispersive p_z band, i.e., a wider bandwidth for the occupied electrons in the CBs. In the previous GW band-structure calculations for BN sheet[22] and h-BN,[23] the effect of many-body correction to the bottom of CBs is mainly in shifting the band energy rather than their curvatures. These results would support our above conclusions as the join/disjoin of the p_z and the s band as well as the curvature of the p_z band dominate the crucial physics of magnetism in O_N and Si_B.

The establishment of the polarized itinerant electrons in O_N at $x=1/4$ is further supported through the charge distribution for the states in CBs just below E_F around Γ point in the nonspin-polarized calculation. In O_N, the charges distribute mainly on the B atoms surrounding the O impurity (a rather extending distribution) which is further joined by the charges distributing above the more distant N atoms. Therefore, the charges distribute as connected charge sheet throughout the system for the isosurface of density less than $0.324e$.[24] This result contrasts to that in the Si_B system whose charges distribute mostly around the substitute Si atoms (a more local distribution) and the connected isosurface occur only when the density is less than $0.213e$.

The x-dependent MEs are also very different for Si_B and O_N. In Si_B, both the ME_{FM} and the ME_{AFM} decreases monotonically with respect to increasing x (decreasing d_{nn}). However, in O_N, the two x-dependent MEs diverge at values of x larger than 1/16, i.e., the decreasing and approaching zero ME_{AFM} versus an increasing ME_{FM}. We should emphasize here that the behavior of ME_{FM} for O_N differs not only from that for Si_B but also from that for the systems carrying localized moments formed by other nonmagnetic substitute atoms in the BN sheet. Examples are the 2D BN sheet with carbon atoms substituting for either B or N atom, Si atoms for N atoms, as well as the vacancies created by removing either B or N atom.[10] The exceptional behavior of ME_{FM} together with the vanishing ME_{AFM} in O_N provides a prominent feature for this 2D system as developing into the polarized itinerant electron phase.

IV. ROBUSTNESS OF THE POLARIZED ITINERANT ELECTRONS IN O_N

In order to examine how the establishment of the polarized itinerant electrons in O_N at $x=1/4$ depends on the oxygen distributions, different supercells consisting of O atoms with the same nearest-neighbor distance $d_{nn} \sim 5$ Å but different numbers and distributions are studied. They include (a) a 6×6 supercell but with only eight instead of nine O substitute atoms, (b) a 4×4 supercell but with only three instead of four O atoms, and (c) a rectangular instead of a 4×2 hexagonal supercell with two O substitute atoms. All these examined systems were found to be still stabilized in the polarized itinerant electron phase with less than 4 meV changes in ME_{FM}. Regarding the substitute-atom concentration x, the highest x of magnetic O_N system we considered is 1/3, i.e., $d_{nn}=4.3$ Å. At this concentration, the system re-
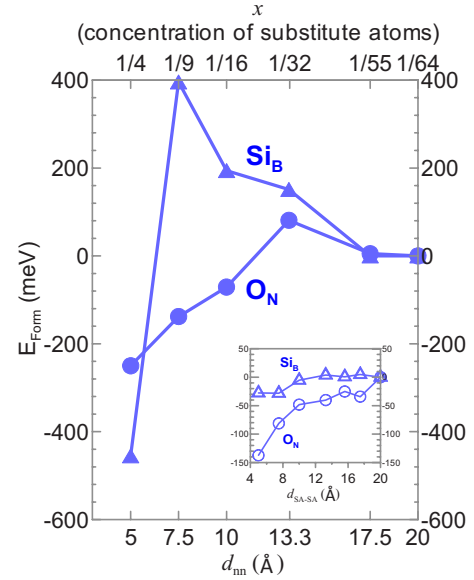

FIG. 3. (Color online) The x-dependent formation energy for O_N and Si_B, where the reference zero is chosen as the formation energy at $x=1/64$, i.e., $d_{nn}=20$ Å.

mains stabilized in the polarized itinerant electron phase. However, we should emphasize that the role of N atoms in O_N is essential as magnetism would disappear if all N atoms in a BN sheet are replaced by O atoms, i.e., the BO sheet is in fact a normal metal. When mapping into the 2D HEG, this corresponds to the paramagnetic fluid at high electron density.

Figure 3 shows the x-dependent formation energy for O_N and Si_B, which is defined as

$$E_{Form} \equiv E_{O_N(Si_B)} - E_{BN\ sheet} + E_{N(B)} - E_{O(Si)},$$

where $E_{O_N(Si_B)}$ and $E_{BN\ sheet}$ are the energies for the O_N (Si_B) system (ferromagnetically polarized ones) and the BN sheet calculated by using exactly the same supercell to eliminate numerical errors, E_N (E_B) and E_O (E_{Si}) are the energies for the removed N (B) and the added O (Si) atoms, respectively.[25] The formation energy for the system of $x=1/64$, i.e., the system with no interaction among the substitute atoms, is taken as the reference zero in the figure. Unlike the repulsive interactions in Si_B at $x \leq 1/9$, the O atoms introduced for substituting N atoms in the BN sheet exhibit attractive interaction once x becomes larger than 1/32. Besides, by employing a very large supercell (11×10) with only two SAs created at the distance d_{SA-SA} in the cell, it is shown (see the inset in Fig. 3) that for both systems, the substitute atoms tend to aggregate to form the system of $x=1/4$.

Considering the possible experimental fabrication of this 2D system supported on a substrate, our study show that the system with polarized itinerant electrons can sustain an external applied tensile and compressive strain of up to 0.1, i.e., a change of 10% in lattice constant. Similar study for Si_B, on the contrary, leads to a nonmagnetic state when the system is under compressive strain.

V. CONCLUSION

In summary, we have explored the possible magnetic phases in O_N and Si_B systems using first-principles method. The polarized itinerant electron phase was found in the $BN_{3/4}O_{1/4}$ system while in the Si_B system, only the paramagnetic phase at low silicon concentrations and ferromagnetic phase at high silicon concentrations were identified. The different magnetic properties in O_N and Si_B were discussed through the x-dependent magnetization energy, the band structures, and the charge-density distributions. The robustness of the formation of the polarized itinerant electron phase was also discussed with respect to the O substitute-atom distributions and the applied strain to the system.

*fmliu@phys.ncku.edu.tw; ru-fen.liu@crm2.uhp-nancy.fr

†ccheng@mail.ncku.edu.tw

[1] K. S. Novoselov, D. Jiang, F. Schedin, T. J. Booth, V. V. Khotkevich, S. V. Morozov, and A. K. Geim, Proc. Natl. Acad. Sci. U.S.A. **102**, 10451 (2005).

[2] C. Jin, F. Lin, K. Suenaga, and S. Iijima, Phys. Rev. Lett. **102**, 195505 (2009).

[3] D. M. Ceperley, Nature (London) **397**, 386 (1999).

[4] B. Tanatar and D. M. Ceperley, Phys. Rev. B **39**, 5005 (1989).

[5] C. Attaccalite, S. Moroni, P. Gori-Giorgi, and G. B. Bachelet, Phys. Rev. Lett. **88**, 256601 (2002).

[6] N. D. Drummond and R. J. Needs, Phys. Rev. Lett. **102**, 126402 (2009).

[7] E. P. Wigner, Phys. Rev. **46**, 1002 (1934).

[8] N. G. Chopra, R. J. Luyken, K. Cherrey, V. H. Crespi, M. L. Cohen, S. G. Louie, and A. Zettl, Science **269**, 966 (1995).

[9] Z.-G. Chen, J. Zou, G. Liu, F. Li, Y. Wang, L. Wang, X.-L. Yuan, T. Sekiguchi, H.-M. Cheng, and G. Q. Lu, ACS Nano **2**, 2183 (2008).

[10] R.-F. Liu and C. Cheng, Phys. Rev. B **76**, 014405 (2007).

[11] V. Barone and J. E. Peralta, Nano Lett. **8**, 2210 (2008).

[12] P. Hohenberg and W. Kohn, Phys. Rev. **136**, B864 (1964); W. Kohn and L. J. Sham, *ibid.* **140**, A1133 (1965).

[13] J. P. Perdew, in *Electronic Structure of Solids' 91*, edited by P. Ziesche and H. Eschrig (Akademie-Verlag, Berlin, 1991); J. P. Perdew, J. A. Chevary, S. H. Vosko, K. A. Jackson, M. R. Pederson, D. J. Singh, and C. Fiolhais, Phys. Rev. B **46**, 6671 (1992).

[14] P. E. Blöchl, Phys. Rev. B **50**, 17953 (1994).

[15] G. Kresse and D. Joubert, Phys. Rev. B **59**, 1758 (1999).

[16] Vienna *ab initio* simulation package, G. Kresse and J. Hafner, Phys. Rev. B **47**, 558 (1993); **49**, 14251 (1994); G. Kresse and J. Furthmuller, Comput. Mater. Sci. **6**, 15 (1996); Phys. Rev. B **54**, 11169 (1996).

[17] H. J. Monkhorst and J. D. Pack, Phys. Rev. B **13**, 5188 (1976).

[18] H. Hellmann, *Einführung in die Quantenchemie* (Deuticke, Leipzig, 1937), pp. 61 and 285; R. P. Feynman, Phys. Rev. **56**, 340 (1939).

[19] A class of the doped systems involving only $2s$ and $2p$ electrons in the host 2D BN sheet has been studied previously (Ref. 10) in which two types of magnetic moments are identified, i.e., the planer one formed by sp^2 electrons and the perpendicular one formed by p_z electrons. The structure likely undergoes distortions for the systems with planer magnetic moments, besides we further found that their moments tend to vanish at $x=1/4$ while that for the systems with perpendicular magnetic moments likely stays in the threefold symmetry.

[20] Contrary to the invariable magnetic moments of $1\mu_B$ by the substituted O and Si atoms in a BN sheet, the magnetic moments by substituting B and N atoms in graphene disappear at low substitution concentration (Ref. 21). This could be attributed to the unusual linear dispersion π and π^* bands joined at the K symmetry point in reciprocal space in graphene.

[21] R. Singh and P. Kroll, J. Phys.: Condens. Matter **21**, 196002 (2009).

[22] X. Blase, A. Rubio, S. G. Louie, and M. L. Cohen, Phys. Rev. B **51**, 6868 (1995).

[23] B. Arnaud, S. Lebègue, P. Rabiller, and M. Alouani, Phys. Rev. Lett. **96**, 026402 (2006).

[24] The distance between two layers in the bulk hexagonal BN, i.e., 3.3 Å, were used to determine the isocharge density.

[25] There are probably more appropriate choices for $E_{N(B)}$ and $E_{O(Si)}$, e.g., half of the energy of O_2 for E_O. However, as we are discussing the formation energy relative to that of the systems with $x=1/64$, the systems with those terms are canceled out and play no role here.